Published in final edited form as:
Vision Res. 2011 January 28; 51(2): 243–250. doi:10.1016/j.visres.2010.08.003.

Dendrite Plasticity in the Lateral Geniculate Nucleus in Primate Glaucoma

Tina Ly[1], **Neeru Gupta**[1,2,3], **Robert N. Weinreb**[4], **Paul L. Kaufman**[5], and **Yeni H. Yücel**[1,3]

[1]Ophthalmology & Vision Sciences, Laboratory Medicine & Pathobiology, St. Michael's Hospital, University of Toronto, Toronto, Ontario, Canada

[2]Glaucoma & Nerve Protection Unit, St. Michael's Hospital, Toronto, Ontario, Canada

[3]Keenan Research Centre at the Li Ka Shing Knowledge Institute of St. Michael's Hospital, Toronto, Ontario, Canada

[4]Hamilton Glaucoma Center, University of California, San Diego, California, United States

[5]Department of Ophthalmology and Vision Sciences, University of Wisconsin, Madison, Wisconsin, United States

Abstract

Neural degeneration in glaucoma involves retinal ganglion cells and neurons of their major target, the lateral geniculate nucleus (LGN). Dendrites of relay LGN neurons projecting to the visual cortex were studied by immunocytochemical and quantitative Sholl analysis in combination with confocal microscopy and 3D-morphometry. In non-human adult primate glaucoma, relay LGN neurons showed reduced dendrite complexity and length, and these changes were modified by NMDA receptor blockade. Dendrite plasticity of LGN relay neurons in adult primate glaucoma has implications for potential disease modification by treatment interventions.

Keywords

neuroprotection; transsynaptic degeneration; neurodegeneration; glutamate; NMDA

1. INTRODUCTION

Glaucoma is a major cause of irreversible blindness worldwide, characterized by retinal ganglion cell (RGC) loss (Weinreb & Khaw, 2004). Degeneration of retinal ganglion cells spreads transsynaptically to their main target, the lateral geniculate nucleus (LGN) of the brain in human glaucoma (Gupta et al., 2006, Gupta et al., 2008). Previous studies in experimental primate glaucoma, show degenerative changes in the LGN including neuron loss, (Yucel et al., 2000, Weber, Chen, Hubbard & Kaufman, 2000), neuron atrophy (Weber,

Corresponding Author: Dr. Yeni H. Yücel, St. Michael's Hospital, 30 Bond Street, Shuter Wing, 5-038, Toronto Ontario M5B 1W8, Phone: 416 864-6060 x 6755, Fax: 416 864-5648 yeni.yucel@utoronto.ca.

DISCLOSURE

Drs. Y. H. Yücel, N. Gupta, R.N. Weinreb and P.L. Kaufman are consultants to Allergan Inc. Dr. N. Gupta and R.N. Weinreb were investigators for the memantine clinical trial that ended in 2006 (Allergan Inc).

Chen, Hubbard & Kaufman, 2000, Yucel, Zhang, Weinreb, Kaufman & Gupta, 2001), reactive gliosis (Sasaoka et al., 2008), and microglial activation (Imamura et al., 2009). Neuron loss and atrophy increase with increasing RGC loss as do metabolic changes observed in the visual cortex in primate glaucoma. (Yucel et al., 2000, Yucel et al., 2001, Yucel et al., 2003).

Dendrites are fine processes emerging from the cell body of neurons that form elaborate dendritic arbors supporting post-synaptic contact elements (Johnston & Narayanan, 2008). Disturbances to dendrite branching can disrupt neural network organization and lead to neural dysfunction, as in human neurological disorders including Alzheimer's disease (Moolman, Vitolo, Vonsattel & Shelanski, 2004). Their fine structure is maintained by microtubules, and among the associated proteins, microtubule-associated protein-2 (MAP2) is enriched in dendrites (Cassimeris & Spittle, 2001, Ichihara et al., Kitazawa, Iguchi, Hotani & Itoh, 2001) playing an important role in dendrite morphology and branching (Dehmelt & Halpain, 2005, Harada et al., 2002, Matus, 1994). MAP2 has been used as a marker to assess dendrites in neurodegenerative diseases (Goedert, Crowther & Garner, 1991, Kaufmann, Naidu & Budden, 1995, Kwei, Jiang & Haddad, 1993, Matesic & Lin, 1994).

In glaucoma, dendrites in the primate retina undergo atrophy (Weber, Kaufman & Hubbard, 1998, Morgan, Uchida & Caprioli, 2000). A study in which LGN interneurons confined to the LGN and relay neurons projecting to the visual cortex were not discriminated, showed dendrite changes in primate glaucoma (Gupta et al., 2007). However, detailed dendrite evaluation of the LGN relay neurons under conditions of glaucoma at various stages of disease and following pharmacological treatment has not been previously investigated. Memantine is an NMDA glutamate open-channel blocker approved as a neuroprotective agent for the treatment of cognitive impairment in Alzheimer's disease (Reisberg et al., 2003). The purpose of this work is to identify and quantify dendrite characteristics of LGN relay neurons in a primate model of glaucoma to determine whether they are altered, and if so, whether these changes are modifiable by memantine (Bormann, 1989).

2. MATERIAL AND METHODS

2.1 Subjects

All experiments were performed following the guidelines of the Association for Research in Vision and Ophthalmology Resolution on the Use of Animals in Research.

Six LGNs from six normal adult cynomolgus monkeys (*Macaca fascicularis*) from the University of Wisconsin, Madison were used as controls. They were perfused intracardiacly with 4% paraformaldehyde in 0.1 M phosphate buffer (pH 7.4). Intraocular pressure (IOP) measurements were performed *in vivo* before sacrifice with a pneumatonometer (Digilab, Norwell, MA) under light sedation (intramuscular injection of 5 mg/kg of ketamine hydrochloride) and topical anesthesia (5% proparacaine hydrochloride) (Yucel et al., 2000). The mean IOP ranged from 12.3 to 21.0 mm Hg and the maximum IOP ranged from 13.0 to 26.0 mm Hg. There was significant difference in mean IOP ($P < 0.001$) or maximum IOP ($P < 0.001$) between the vehicle-treated glaucoma group and normal group.

Experimental glaucoma was induced in adult monkeys (*Macaca fascicularis*) by laser scarification of the trabecular meshwork (Hare et al., 2004). The duration of IOP elevation was 14 months. Three animals out of 18 were excluded from the present study due to either suboptimal fixation or unidentifiable LGN layers. Two groups of monkeys were evaluated and compared: 1) 7 vehicle-treated (VT) monkeys with glaucoma and 2) 8 memantine-treated (MT) monkeys with glaucoma who received a daily oral dose of 4 mg/kg of memantine. In both the VT and MT glaucoma groups, the treatment was continued during

14 months until sacrifice (Hare, et al. 2004). There was no significant difference in mean IOP ($P = 0.43$) or maximum IOP ($P = 0.73$) between the VT and MT glaucoma groups (Yucel et al., 2006a). Previously published optic nerve counts of these animals showed no significant difference in mean percent optic nerve fiber loss between the VT and MT glaucoma groups (Yucel et al., 2006a).

2.2 Tissue processing

Perfusion fixation under deep general anesthesia and tissue processing and 40 micron-thick serial sections were performed (Yucel et al., 2000). Every seventh section was mounted onto a glass slide and stained with cresyl violet. Care was taken to use the same tissue processing procedures for all monkey brains. Sections containing left LGN with six layers were randomly selected for each of the normal control animals and each of the VT and MT glaucoma animals.

2.3 Double immunofluorescence labeling of MAP2 and parvalbumin

LGN sections were double-labeled with a monoclonal antibody against MAP2 (Clone HM-2, Sigma, St. Louis, MO), and a polyclonal antibody against parvalbumin (PV28, Swant, Bellinzona, Switzerland), a calcium-binding protein, a specific marker for relay LGN neurons (Johnson & Casagrande, 1995). The tyramide signal amplification (TSA) kit (Invitrogen Inc., ON, Canada) was used to enhance immunostaining. Sections were washed with phosphate buffered saline (1 × PBS, 3 × 10 min). All subsequent washes were performed with 1 × PBS, pH 7.35 (3 × 5 min). Sections were incubated with 0.2% Triton-X (Sigma, St. Louis, MO) in PBS (2 × 5 min). After PBS wash, endogenous peroxidase activity was quenched by 3% H_2O_2 (2 × 15 min). Sections were washed with PBS and blocked in 1% blocking reagent (TSA kit). Incubation in parvalbumin [1:500] was extended to 2 hours at room temperature, overnight at 4°C and then left at room temperature for another 2 hours. Sections were washed with PBS and incubated in anti Rabbit-HRP [1:100] (TSA kit). After PBS wash, sections were incubated in Tyramide-Alexa Fluor-488 diluted in Amplification Buffer [1:100] (2×10min). Sections were washed with PBS, quenched with 3% H_2O_2 (2×15min), and blocked in 1% blocking reagent. Incubation in MAP2 [1:100] was extended to 2 hours at room temperature, overnight at 4°C and then left at room temperature for another 2 hours. Sections were washed with PBS and incubated in anti Mouse-HRP [1:100] (TSA kit). After being washed again in PBS, sections were incubated in Tyramide-Alexa Fluor-555 [1:100] (2×10min) diluted in Amplification buffer (TSA kit). Sections were washed again with PBS, mounted with antifade PVA-DABCO onto Vectabond (Vector Laboratories, Burlingame, CA) coated slides and cover-slipped. Immunostaining experiments for all three groups were performed simultaneously with same reagents. Negative controls were obtained by omitting the primary antibodies.

2.4. Morphological assessment

Immunofluorescence-labeled sections were viewed using an Olympus bright field BX51 upright microscope with a color digital camera (Microfire, Optronics Inc. Goleta, CA) and a computer monitor. The LGN layers were identified as layer 1 to layer 6 from ventral to dorsal. The ventral layers 1 and 2 are magnocellular layers, while the remaining dorsal layers 3–6 are parvocellular layers. Layers 1, 4 and 6 of the left LGN are connected to the glaucomatous right eye while layers 2, 3 and 5 are connected to the non-glaucomatous left eye. We analyzed MAP2-immunoreactive dendrites of parvalbumin-positive relay neurons projecting to the primary visual cortex (Johnson & Casagrande, 1995), located in left LGN magnocellular layer 1 and parvocellular layer 6 connected to the glaucomatous right eye.

2.5. Quantitative analysis

Confocal image acquisition—Sections from MT and VT glaucoma groups, and normal controls were examined using LaserSharp 2000 software (Biorad Cell Science Division, Hernelhempstead, UK) with a digital camera on an upright confocal laser microscope (Biorad Radiance, Bronx, NY on Nikon E800 Upright Microscope, Melville, NY) in a masked fashion. Five sampling sites of 500 μm × 500 μm within each magnocellular layer 1 and parvocellular layer 6 were selected. Within each sampling site, one stack of images was taken under red (CY3 for MAP2) and green (FITC for parvalbumin) channels separately with a 60× oil-immersion objective at zoom of 1.5× and 512 × 512 pixels by LaserSharp2000 program. Serial stack images of 18 μm depth and 0.5 μm step size were collected using the same camera settings for power, gain, iris aperture size, and offset to maintain consistent settings for comparison. All images were obtained using a Kalman filter with 3 passes.

Automated tracing and 3D reconstruction—Stacks of images were imported (Neurolucida; MicroBrightField, Inc., Colchester, VT) and neurons were traced with an automated tracing software (AutoNeuron, MicroBrightField Inc., Colchester, VT). Tracing of MAP2-immunoreactive dendrites (CY3 channel) and parvalbumin-immunostained cell bodies (FITC channel) of stacks of confocal images was performed separately. Two modes of the automated tracing software were used to trace neurons: interactive mode for MAP2-immunostained dendrites, and automatic mode for parvalbumin-immunostained cell bodies. Configuration parameters used for tracing for each neuron were: (1) maximum process diameter, 1.5 μm, (2) ignore somas smaller than, 2.0 μm, (3) soma detector sensitivity, 55 and 65 for layer 1 and layer 6, respectively, and (4) interactive mode.

Quantitative analysis of dendrites—Immunofluorescence labeling, image acquisition and quantitative analysis of the dendrites were performed in a masked fashion. Tracings were loaded into Neurolucida software (NeuroExplorer, MicroBrightField Inc. VT, USA). A total of 45 parvalbumin-positive neurons with MAP2-immunostained dendrites were selected randomly from each magnocellular layer 1 and parvocellular layer 6 per animal for dendrite complexity analysis (Sholl Analysis, NeuroExplorer) and dendrite length analysis (Branch Structure Analysis, NeuroExplorer). In Sholl Analysis, once the cell body to study was selected, the intersections of dendrites and series of spheres with radii 1–14μm, spaced at 1-μm increments, were generated by the software around the cell body. The number of dendrite-sphere intersections to estimate dendrite complexity was calculated by the software. The percent decrease in dendrite complexity was calculated from the difference between the average mean dendrite complexity of the normal group and mean dendrite complexity of MT and VT animals with glaucoma divided by the average mean of dendrite complexity in the normal group. Percent decrease in dendrite length was assessed in a similar manner.

2.6. Statistical analysis

The two-tailed student *t*-test was used to compare dendrite parameters in relay neurons in LGN layers 1 and 6 of the VT glaucoma group to the MT glaucoma group, and to the normal control group. Mean IOP, maximum IOP, and percent optic nerve fiber loss were also compared using a *t*-test.

Using the generalized linear models procedure of SAS statistical software (SAS Institute Inc, Cary, NC), percent decrease in dendrite complexity and dendrite length were compared between the memantine- and vehicle-treated glaucoma groups, with mean IOP as a covariate.

3. RESULTS

3.1. Dendritic plasticity in LGN relay neurons in experimental glaucoma (Figure 1)

MAP2-immunoreactivity in magnocellular layer 1 relay neurons in normal monkey (Figure 1A) was more intense compared to vehicle-treated (VT) glaucoma monkeys (Figure 1B). Similar observations were made for parvocellular layer 6 (Figure 1 D, E). MAP2-immunoreactivity in magnocellular layer 1 relay neurons in memantine-treated (MT) glaucoma monkeys (Figure 1C) was more intense compared to VT glaucoma monkeys (Figure 1 B). Similar observations were made for parvocellular layer 6 (Figure 1 E, 1F).

Dendrite complexity (Figure 2) and length were measured in normal group, VT and MT glaucoma groups (Table 1). In magnocellular layer 1, both mean dendrite complexity (Figure 3A) and dendrite length (Figure 3B) were significantly decreased in the VT glaucoma group compared with those in the normal group (11.2 ± 1.0 (Mean ± SD) vs. 23.7 ± 1.5, $P < 0.0001$; 18.4 ± 1.4 μm vs. 38.5 ± 3.1 μm, $P < 0.0001$; respectively).

In parvocellular layer 6, both mean dendrite complexity (Figure 4A) and length (Figure 4B) were significantly decreased in the VT glaucoma group compared with those in the normal group (11.1 ± 1.3 vs. 21.2 ± 0.9, $P < 0.0001$; 16.7 ± 1.9 μm vs. 33.7 ± 2.4 μm, $P < 0.0001$, respectively).

3.2. Dendritic alterations in LGN relay neurons in memantine-treated glaucoma monkeys

3.2.1. Magnocellular layer 1—Percent decrease in dendrite complexity (Table 2) in MT glaucoma was significantly reduced compared to VT glaucoma group (38.1% ± 10.7 vs. 52.9% ± 4.2, $P = 0.0047$; respectively). Percent decrease in dendrite length in MT glaucoma was also significantly reduced compared to VT glaucoma (Table 2).

3.2.2. Parvocellular layer 6—Percent decrease in dendrite complexity (Table 2) in MT glaucoma was significantly reduced compared to VT glaucoma group (33.8% ± 6.7 vs. 47.8% ±6.3, $P = 0.0011$). Percent decrease in dendrite length in MT glaucoma was also significantly reduced compared to VT glaucoma (Table 2).

3.3 Relation with dendritic changes and mean IOP in memantine-treated and vehicle-treated glaucoma groups

3.3.1. Magnocellular Layer 1—Percent decrease in mean dendrite complexity increased with mean IOP for magnocellular layer (Figure 5A) for MT and VT glaucoma groups, and the linear regression of the dendrite complexity decrease on IOP was statistically significant ($P < 0.05$). ANCOVA test, with mean IOP as a covariate, showed significantly less percent decrease in dendrite complexity in the MT glaucoma group compared to the VT glaucoma group ($P = 0.017$).

The linear regression of the dendrite length decrease on IOP was statistically significant (Figure 5B) ($P < 0.05$). ANCOVA test, with mean IOP as a covariate, showed significantly less percent decrease in dendrite dendrite length in the MT compared to the VT group in magnocellular layer 1 ($P = 0.0032$).

3.3.2.Parvocellular Layer 6—Percent decrease in mean dendrite complexity increased with mean IOP for parvocellular layer 6 (Figure 6A) for MT and VT glaucoma groups, and the linear regression of the dendrite complexity decrease on IOP was statistically significant ($P < 0.05$). ANCOVA test, with mean IOP as a covariate, showed significantly less percent decrease in dendrite complexity in the MT compared to the VT group ($P = 0.0003$). The linear regression of the dendrite length decrease on IOP was statistically significant (Figure

6B) ($P < 0.05$). ANCOVA test, with mean IOP as a covariate, showed significantly less percent decrease in dendrite length in the MT compared to the VT group in parvocellular layer 6 ($P = 0.0061$).

4. Discussion

Pathologic changes in dendrites are considered an early sign of neuron injury (Bywood & Johnson, 2000) and the decrease in MAP2 immunostained dendrites is considered an early indicator of neuron injury (Kitagawa et al., 1989, Kwei et al., 1993). Dendrites of relay LGN neurons in normal primate have been rarely studied, (Wilson, 1986, Wilson, 1989), and no detailed quantitative assessment of dendritic parameters are available. A previous study in experimental primate glaucoma with mild optic nerve fiber loss, showed reduction of dendritic complexity and field area in the LGN neurons without distinguishing larger relay neurons from smaller interneurons, (Gupta et al., 2007). The combination of double labeling with MAP2, a dendritic marker and parvalbumin, a cell type specific marker for relay LGN neurons (Johnson & Casagrande, 1995), with confocal microscopy and 3D reconstruction/tracing enabled us to perform the quantitative assessment of dendrites of LGN relay neurons in glaucomatous monkeys in comparison with normal monkeys. This study shows for the first time a decrease in dendrite complexity and in length of specifically the relay LGN neurons in primate glaucoma. Furthermore, this analysis showed that both dendrite complexity and length of relay LGN neurons in glaucoma decreased with mean IOP. Further studies are needed to determine the functional significance of dendritic changes in surviving relay LGN neurons, and their involvement in visual dysfunction in glaucoma. Recent studies in retinae of primate glaucoma showed that retinal ganglion cells were less responsive, both spatially and temporally, to visual stimuli, and that the reduction in visual responsiveness most likely results from significant changes in dendritic architecture (Weber & Harman, 2005).

Blockade of NMDA open channel receptor using memantine attenuated decrease in dendrite complexity and in length in relay LGN neurons in primate glaucoma. Confirmation of these results by ANCOVA analysis using mean IOP as covariate, suggests that the difference between memantine-treated and vehicle-treated groups is not due to differences in mean IOP between groups. Memantine also protected cell body size in the LGN in glaucoma (Yucel et al., 2006a) and this may be in part due to action on NMDA receptors in relay LGN neurons (Jones, Tighilet, Tran & Huntsman, 1998). Memantine may also be acting on the NMDA receptor subtype located in the retina (Grunert, Haverkamp, Fletcher & Wassle, 2002) and the visual cortex (Huntley et al., 1994), each major sources of excitatory input to the LGN (Montero & Wenthold, 1989). Although the expression of NMDAR1 receptor subunit, part of all NMDARs, is increased in LGN layer in primate glaucoma (Yucel et al., 2006b), the expression of other NMDAR subunits (Liu et al., 2007) and the cellular location of NMDARs (synaptic or extrasynaptic) (Hardingham, Fukunaga & Bading, 2002, Sattler et al., 2000) that are implicated in controlling their effect on neuronal viability, are not yet known in normal and glaucomatous LGN. This knowledge may be important to understand the effect of memantine of relay neurons in glaucomatous LGN since memantine has been shown to act preferentially on the extrasynaptic NMDA receptors (Leveille et al., 2008). It is not clear whether the extent of dendritic changes following memantine treatment contributes the decrease in amplitude reduction of visually-evoked cortical potential in memantine-treated glaucoma monkeys (Hare et al., 2004). Memantine failed to demonstrate a neuroprotective treatment effect on visual fields of glaucoma patients in a large clinical trial. Nonetheless, the finding of measurable dendrite plasticity in central visual neurons following administration of memantine suggests that targeting LGN neurons in glaucoma is a strategy worth exploring to prevent visual dysfunction in glaucoma.

Acknowledgments

This work was partially supported by Canadian Institutes of Health Research/Small Medium Enterprise Program (NG, YY) and The Fred Jarvis Fund (NG). We thank Audrey Darabie and Qiang Zhang for excellent technical work. We also acknowledge the contribution of Barbara Thomson, MSc, Department of Statistics, University of Toronto.

REFERENCES

Bormann J. Memantine is a potent blocker of N-methyl-D-aspartate (NMDA) receptor channels. Eur J Pharmacol. 1989; 166(3):591–592. [PubMed: 2553441]

Bywood PT, Johnson SM. Dendrite loss is a characteristic early indicator of toxin-induced neurodegeneration in rat midbrain slices. Exp Neurol. 2000; 161(1):306–316. [PubMed: 10683296]

Cassimeris L, Spittle C. Regulation of microtubule-associated proteins. Int Rev Cytol. 2001; 210:163–226. [PubMed: 11580206]

Dehmelt L, Halpain S. The MAP2/Tau family of microtubule-associated proteins. Genome Biol. 2005; 6(1):204. [PubMed: 15642108]

Goedert M, Crowther RA, Garner CC. Molecular characterization of microtubule-associated proteins tau and MAP2. Trends Neurosci. 1991; 14(5):193–199. [PubMed: 1713721]

Grunert U, Haverkamp S, Fletcher EL, Wassle H. Synaptic distribution of ionotropic glutamate receptors in the inner plexiform layer of the primate retina. J Comp Neurol. 2002; 447(2):138–151. [PubMed: 11977117]

Gupta N, Ang LC, Noel de Tilly L, Bidaisee L, Yucel YH. Human glaucoma and neural degeneration in intracranial optic nerve, lateral geniculate nucleus, and visual cortex. Br J Ophthalmol. 2006; 90(6):674–678. [PubMed: 16464969]

Gupta N, Ly T, Zhang Q, Kaufman PL, Weinreb RN, Yucel YH. Chronic ocular hypertension induces dendrite pathology in the lateral geniculate nucleus of the brain. Exp Eye Res. 2007; 84(1):176–184. [PubMed: 17094963]

Gupta N, Greenberg G, Noel de Tilly L, Gray B, Polemidiotis M, Yucel YH. Atrophy of the Lateral Geniculate Nucleus in Human Glaucoma by Magnetic Resonance Imaging. Br J Ophthalmol. 2009; 93(1):56–60. [PubMed: 18697810]

Harada A, Teng J, Takei Y, Oguchi K, Hirokawa N. MAP2 is required for dendrite elongation, PKA anchoring in dendrites, and proper PKA signal transduction. J Cell Biol. 2002; 158(3):541–549. [PubMed: 12163474]

Hardingham GE, Fukunaga Y, Bading H. Extrasynaptic NMDARs oppose synaptic NMDARs by triggering CREB shut-off and cell death pathways. Nat Neurosci. 2002; 5(5):405–414. [PubMed: 11953750]

Hare WA, WoldeMussie E, Lai RK, Ton H, Ruiz G, Chun T, Wheeler L. Efficacy and safety of memantine treatment for reduction of changes associated with experimental glaucoma in monkey, I: Functional measures. Invest Ophthalmol Vis Sci. 2004; 45(8):2625–2639. [PubMed: 15277486]

Huntley GW, Vickers JC, Janssen W, Brose N, Heinemann SF, Morrison JH. Distribution and synaptic localization of immunocytochemically identified NMDA receptor subunit proteins in sensory-motor and visual cortices of monkey and human. J Neurosci. 1994; 14(6):3603–3619. [PubMed: 8207475]

Ichihara K, Kitazawa H, Iguchi Y, Hotani H, Itoh TJ. Visualization of the stop of microtubule depolymerization that occurs at the high-density region of microtubule-associated protein 2 (MAP2). J Mol Biol. 2001; 312(1):107–118. [PubMed: 11545589]

Imamura K, Onoe H, Shimazawa M, Nozaki S, Wada Y, Kato K, Nakajima H, Mizuma H, Onoe K, Taniguchi T, Sasaoka M, Hara H, Tanaka S, Araie M, Watanabe Y. Molecular imaging reveals unique degenerative changes in experimental glaucoma. Neuroreport. 2009; 20(2):139–144. [PubMed: 19057418]

Johnson JK, Casagrande VA. Distribution of calcium-binding proteins within the parallel visual pathways of a primate (Galago crassicaudatus). J Comp Neurol. 1995; 356(2):238–260. [PubMed: 7629317]

Johnston D, Narayanan R. Active dendrites: colorful wings of the mysterious butterflies. Trends Neurosci. 2008; 31(6):309–316. [PubMed: 18471907]

Jones EG, Tighilet B, Tran BV, Huntsman MM. Nucleus- and cell-specific expression of NMDA and non-NMDA receptor subunits in monkey thalamus. J Comp Neurol. 1998; 397(3):371–393. [PubMed: 9674563]

Kaufmann WE, Naidu S, Budden S. Abnormal expression of microtubule-associated protein 2 (MAP-2) in neocortex in Rett syndrome. Neuropediatrics. 1995; 26(2):109–113. [PubMed: 7566447]

Kitagawa K, Matsumoto M, Niinobe M, Mikoshiba K, Hata R, Ueda H, Handa N, Fukunaga R, Isaka Y, Kimura K, et al. Microtubule-associated protein 2 as a sensitive marker for cerebral ischemic damage--immunohistochemical investigation of dendritic damage. Neuroscience. 1989; 31(2): 401–411. [PubMed: 2797444]

Kwei S, Jiang C, Haddad GG. Acute anoxia-induced alterations in MAP2 immunoreactivity and neuronal morphology in rat hippocampus. Brain Res. 1993; 620(2):203–210. [PubMed: 8369956]

Leveille F, El Gaamouch F, Gouix E, Lecocq M, Lobner D, Nicole O, Buisson A. Neuronal viability is controlled by a functional relation between synaptic and extrasynaptic NMDA receptors. Faseb J. 2008; 22(12):4258–4271. [PubMed: 18711223]

Liu Y, Wong TP, Aarts M, Rooyakkers A, Liu L, Lai TW, Wu DC, Lu J, Tymianski M, Craig AM, Wang YT. NMDA receptor subunits have differential roles in mediating excitotoxic neuronal death both in vitro and in vivo. J Neurosci. 2007; 27(11):2846–2857. [PubMed: 17360906]

Luthra A, Gupta N, Kaufman PL, Weinreb RN, Yucel YH. Oxidative injury by peroxynitrite in neural and vascular tissue of the lateral geniculate nucleus in experimental glaucoma. Exp Eye Res. 2005; 80(1):43–49. [PubMed: 15652525]

Matesic DF, Lin RC. Microtubule-associated protein 2 as an early indicator of ischemia-induced neurodegeneration in the gerbil forebrain. J Neurochem. 1994; 63(3):1012–1020. [PubMed: 8051544]

Matus A. Stiff microtubules and neuronal morphology. Trends Neurosci. 1994; 17(1):19–22. [PubMed: 7511844]

Morgan JE, Uchida H, Caprioli J. Retinal ganglion cell death in experimental glaucoma. Br J Ophthalmol. 2000; 84(3):303–310. [PubMed: 10684843]

Montero VM, Wenthold RJ. Quantitative immunogold analysis reveals high glutamate levels in retinal and cortical synaptic terminals in the lateral geniculate nucleus of the macaque. Neuroscience. 1989; 31(3):639–647. [PubMed: 2574426]

Moolman DL, Vitolo OV, Vonsattel JP, Shelanski ML. Dendrite and dendritic spine alterations in Alzheimer models. J Neurocytol. 2004; 33(3):377–387. [PubMed: 15475691]

Reisberg B, Doody R, Stoffler A, Schmitt F, Ferris S, Mobius HJ. Memantine in moderate-to-severe Alzheimer's disease. N Engl J Med. 2003; 348(14):1333–1341. [PubMed: 12672860]

Sasaoka M, Nakamura K, Shimazawa M, Ito Y, Araie M, Hara H. Changes in visual fields and lateral geniculate nucleus in monkey laser-induced high intraocular pressure model. Exp Eye Res. 2008; 86(5):770–782. [PubMed: 18378230]

Sattler R, Xiong Z, Lu WY, MacDonald JF, Tymianski M. Distinct roles of synaptic and extrasynaptic NMDA receptors in excitotoxicity. J Neurosci. 2000; 20(1):22–33. [PubMed: 10627577]

Weber AJ, Kaufman PL, Hubbard WC. Morphology of single ganglion cells in the glaucomatous primate retina. Invest Ophthalmol & Vis Sci. 1998; 39(12):2304–2320. [PubMed: 9804139]

Weber AJ, Chen H, Hubbard WC, Kaufman PL. Experimental glaucoma and cell size, density, and number in the primate lateral geniculate nucleus. Invest Ophthalmol Vis Sci. 2000; 41(6):1370–1379. [PubMed: 10798652]

Weber AJ, Harman CD. Structure-function relations of parasol cells in the normal and glaucomatous primate retina. Invest Ophthalmol Vis Sci. 2005; 46(9):3197–3207. [PubMed: 16123419]

Weinreb RN, Khaw PT. Primary open-angle glaucoma. Lancet. 2004; 9422(363):1711–1720. [PubMed: 15158634]

Wilson JR. Synaptic connections of relay and local circuit neurons in the monkey's dorsal lateral geniculate nucleus. Neurosci Lett. 1986; 66(1):79–84. [PubMed: 3714116]

Wilson JR. Synaptic organization of individual neurons in the macaque lateral geniculate nucleus. J Neurosci. 1989; 9(8):2931–2953. [PubMed: 2769372]

Yucel YH, Zhang Q, Gupta N, Kaufman PL, Weinreb RN. Loss of neurons in magnocellular and parvocellular layers of the lateral geniculate nucleus in glaucoma. Arch Ophthalmol. 2000; 118(3): 378–384. [PubMed: 10721961]

Yucel YH, Zhang Q, Weinreb RN, Kaufman PL, Gupta N. Atrophy of relay neurons in magno- and parvocellular layers in the lateral geniculate nucleus in experimental glaucoma. Invest Ophthalmol Vis Sci. 2001; 42(13):3216–3222. [PubMed: 11726625]

Yucel YH, Zhang Q, Weinreb RN, Kaufman PL, Gupta N. Effects of retinal ganglion cell loss on magno-, parvo-, koniocellular pathways in the lateral geniculate nucleus and visual cortex in glaucoma. Prog Retin Eye Res. 2003; 22(4):465–481. [PubMed: 12742392]

Yucel YH, Gupta N, Zhang Q, Mizisin AP, Kalichman MW, Weinreb RN. Memantine protects neurons from shrinkage in the lateral geniculate nucleus in experimental glaucoma. Arch Ophthalmol. 2006a; 124(2):217–225. [PubMed: 16476892]

Yucel Y, Darabie A, Wang S, Kaufman PL, Gupta N. Glutamate NMDA receptor 1 subunit expression is increased in the lateral geniculate nucleus of experimental glaucoma. Invest. Ophthalmol. Vis. Sci. 2006b; 47:1555.

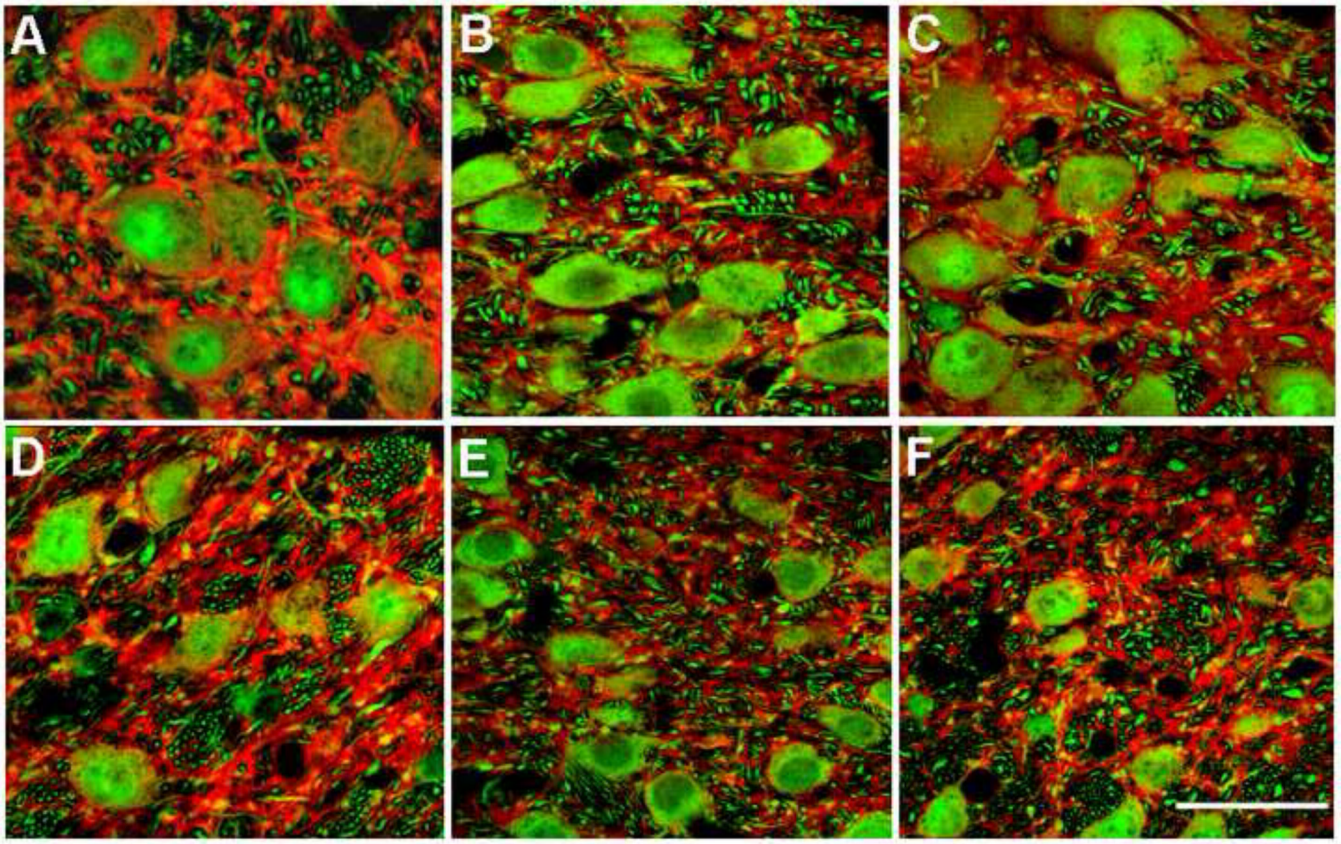

Figure 1.

Projected images of stacks of confocal images of LGN relay neurons immunostained with parvalbumin (green) and dendrites with MAP2 (red). A, B and C show neurons in magnocellular layer 1 from normal monkey ID #S1, from vehicle-treated (VT) glaucoma monkey #106 and from memantine-treated (MT) glaucoma monkey #97, respectively (Table 1). MAP2 immunoreactivity in normal layer 1 (A) was more intense compared to those in the VT glaucoma (B) and MT glaucoma (C) monkeys. In layer 1, MAP2 appeared more intense in MT glaucoma (C) compared to VT glaucoma monkeys (B). Similar results were seen in parvocellular layer 6 in normal (D), VT glaucoma (E) and MT glaucoma (F) monkeys. Scale bar indicates 40 μm.

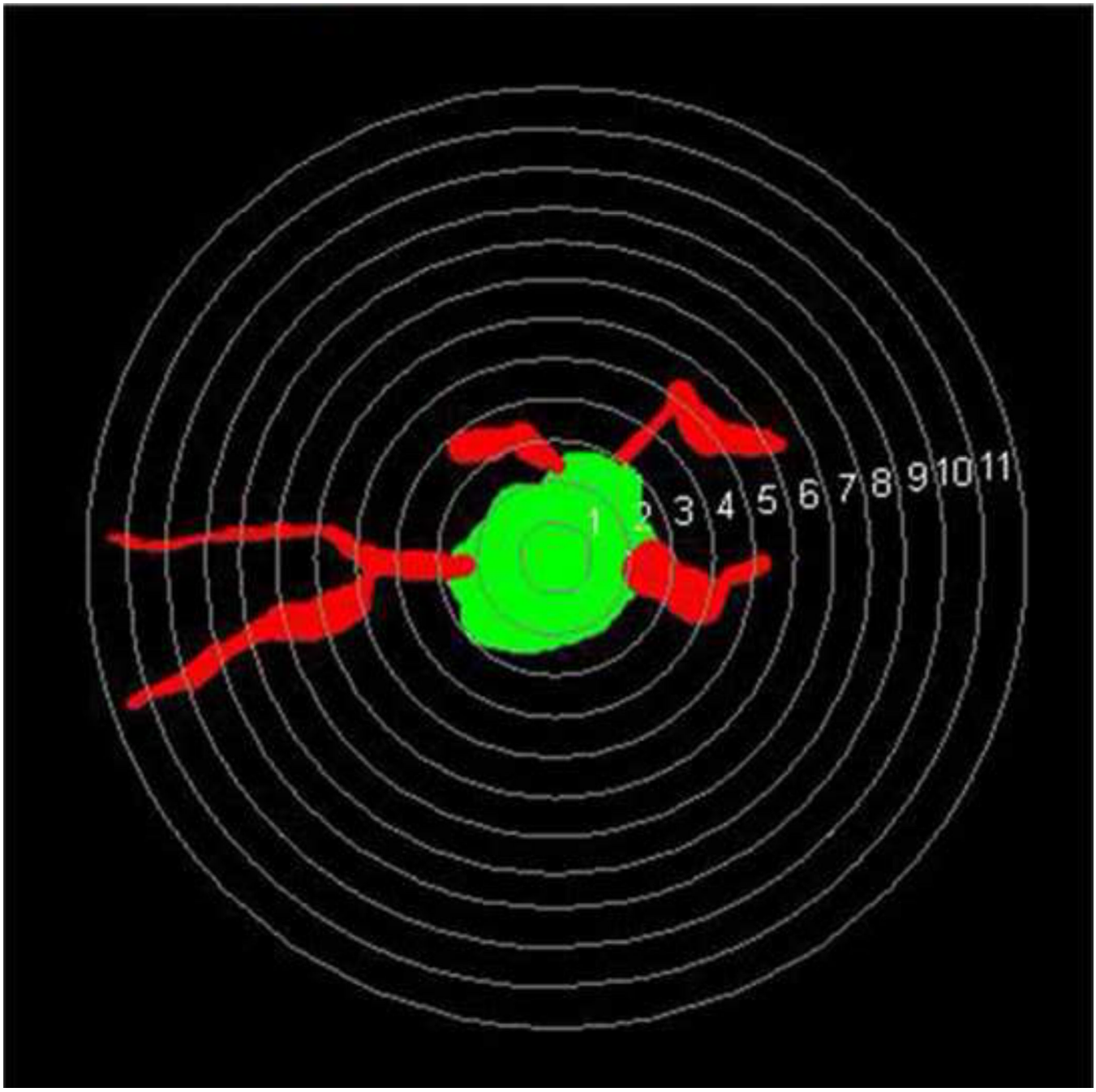

Figure 2.

A randomly selected parvalbumin-positive neuron with MAP2-positive dendrites selected from layer 6 from normal monkey S1 for dendritic complexity analysis is shown. Concentric spheres with different radii (1–11μm) with intervals of 0.5 μm are placed on the cell and its dendrites. The intersections between these circles and dendrites are used to analyze the complexity of dendritic arborization. (Sholl analysis, Neuroexplorer, Colchester, VT).

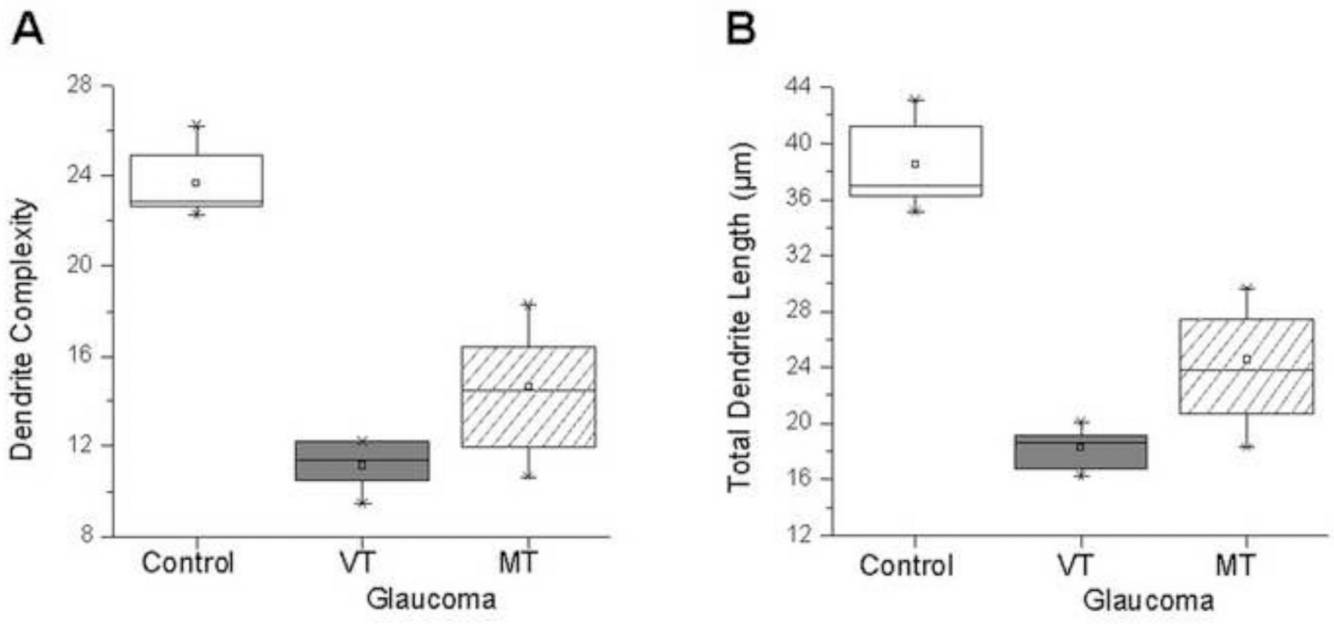

Figure 3.

Magnocellular layer 1: Box plots for dendrite complexity (A) and dendrite length (B) in the normal group, and vehicle-treated (VT) and memantine-treated (MT) glaucoma groups. Compared to normal group, dendrite complexity and dendrite length were reduced in VT glaucoma group. Dendrite complexity and dendrite length in MT group were significantly increased compared to VT group ($P = 0.0048$ and $P = 0.0022$, respectively). The box extends from the 25th percentile to the 75th percentile, with horizontal solid line and square at the median and mean, respectively. The bars indicate the highest and lowest values determined by the 25^{th} and 75^{th} percentiles.

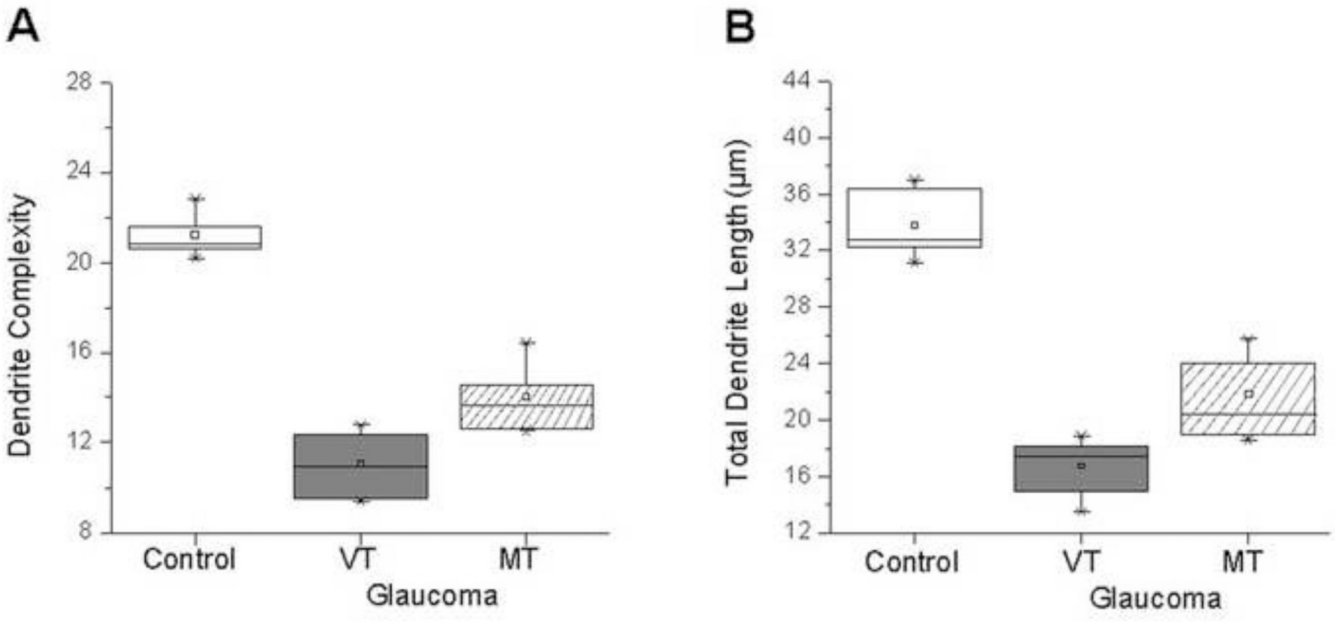

Figure 4.

Parvocellular layer 6: Box plots for dendrite complexity (A) and dendrite length (B) in the normal group, and VT and MT glaucoma groups. Compared to normal group, dendrite complexity and dendrite length were reduced in VT glaucoma group. Dendrite complexity and dendrite length in MT glaucoma group were significantly increased compared to VT glaucoma group ($P = 0.0011$; $P = 0.0012$, respectively). The box extends from the 25th percentile to the 75th percentile, with horizontal solid line and square at the median and mean, respectively. The bars indicate the highest and lowest values determined by the 25^{th} and 75^{th} percentiles.

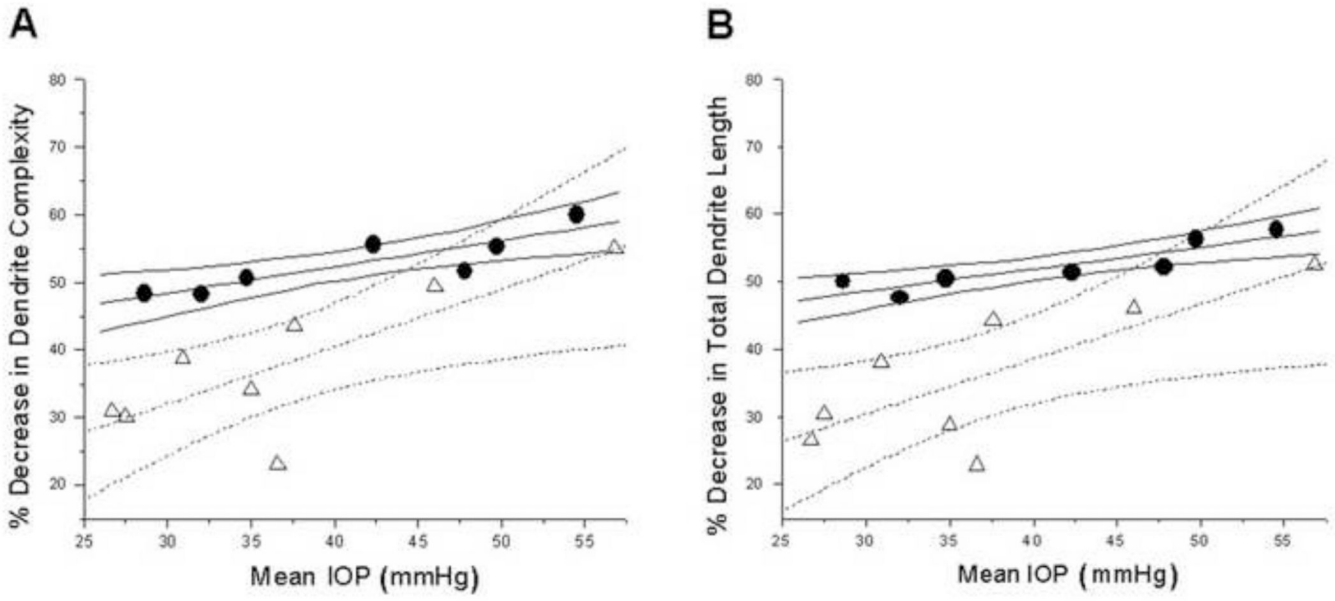

Figure 5.

Magnocellular layer 1: Plots of percent dendrite complexity reduction (A) and percent dendrite length reduction (B) as a function of mean IOP. Triangles and circles indicate percent decrease in dendrite complexity in MT glaucoma group and VT glaucoma group, respectively. (A) Dotted and solid and lines represent linear fit and 95% confidence intervals for the MT and VT glaucoma groups, respectively. Percent decrease in dendrite complexity increased with elevated mean IOP. Similar results were obtained when percent dendrite length reduction was assessed (B)

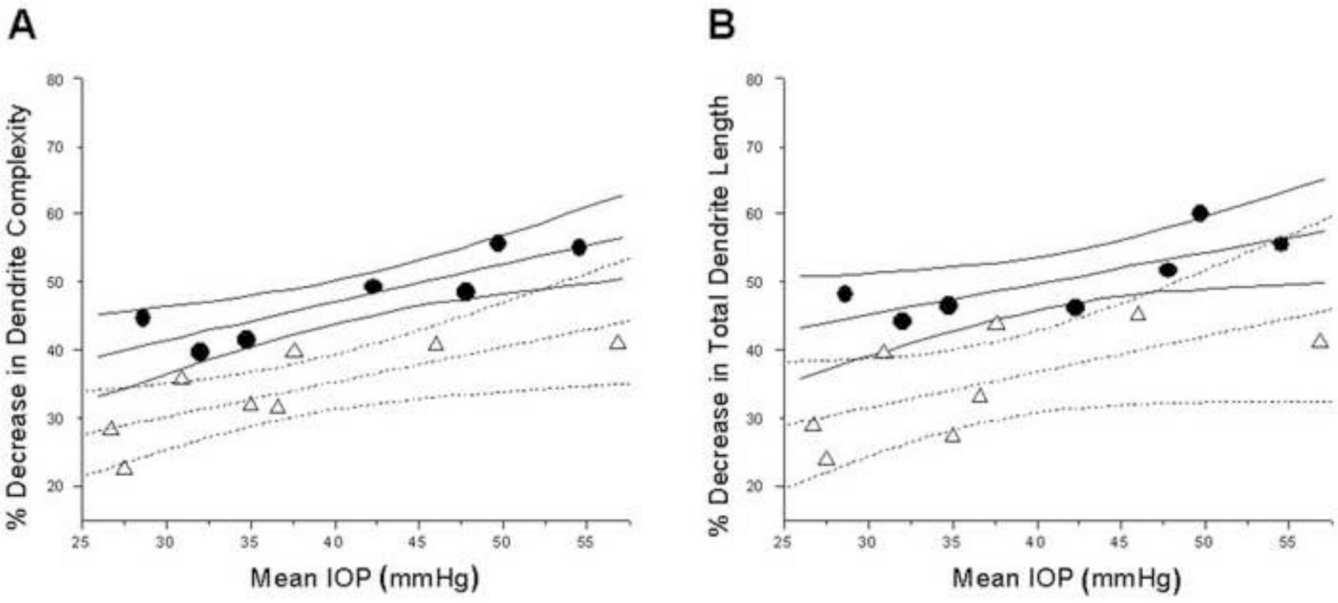

Figure 6.

Parvocellular layer 6: Plots of percent dendrite complexity reduction (A) and percent dendrite length reduction (B) as a function of mean IOP. Triangles and circles indicate percent decrease in dendrite complexity in MT glaucoma group and VT glaucoma group, respectively. (A) Dotted and solid and lines represent linear fit and 95% confidence intervals for the MT glaucoma and VT glaucoma groups, respectively. Percent decrease in dendrite complexity increased with elevated mean IOP. Similar results were obtained when percent dendrite length reduction was assessed (B).

Table 1

Dendritic parameters of LGN relay neurons in normal monkeys, and vehicle-treated (VT) glaucoma and memantine-treated (MT) glaucoma monkeys

	Dendrite complexity, Mean ± SD		Total dendrite length, μm Mean ± SD	
Group, ID	**Layer 1**	**Layer 6**	**Layer 1**	**Layer 6**
Normal				
S1	22.3 ± 4.1	22.8 ± 5.7	35.1 ± 6.7	36.4 ± 9.1
S2	22.9 ± 4.9	21.6 ± 4.7	38.5 ± 8.0	31.1 ± 7.4
S4	22.7 ± 4.3	20.2 ± 3.8	37.0 ± 7.2	33.0 ± 6.9
S6	26.2 ± 6.2	20.6 ± 4.4	43.1 ± 10.7	32.7 ± 6.5
S7	23.2 ± 4.8	20.8 ± 5.6	36.2 ± 7.3	37.0 ± 9.1
S10	24.9 ± 4.7	21.3 ± 4.6	41.1 ± 8.3	32.2 ± 7.7
Mean ± SD	23.7 ± 1.5	21.2 ± 0.9	38.5 ± 3.1	33.7 ± 2.4
Vehicle-treated glaucoma				
91	11.4 ± 4.7	10.9 ± 4.4	18.4 ± 6.9	16.3 ± 6.1
92	9.5 ± 3.1	9.5 ± 2.9	16.2 ± 5.8	15.0 ± 3.9
93	10.6 ± 3.2	9.4 ± 2.8	16.8 ± 5.5	13.5 ± 4.5
96	10.5 ± 4.2	10.7 ± 3.0	18.7 ± 6.2	18.1 ± 5.4
98	11.7 ± 4.5	12.4 ± 4.5	19.0 ± 7.1	18.0 ± 6.8
105	12.2 ± 5.2	11.7 ± 4.1	19.2 ± 7.2	17.4 ± 6.5
106	12.2 ± 4.6	12.8 ± 4.2	20.1 ± 7.2	18.8 ± 6.8
Mean ± SD	11.2 ± 1.0	11.1 ± 1.3	18.4 ± 1.4	16.7 ± 1.9
P value[(a)]	*< 0.0001*	*< 0.0001*	*< 0.0001*	*< 0.0001*
Memantine-treated glaucoma				
94	18.2 ± 6.2	14.6 ± 6.0	29.7 ± 8.5	22.6 ± 9.3
95	12.0 ± 3.3	12.6 ± 3.6	21.0 ± 6.4	18.6 ± 5.4
97	15.6 ± 6.9	14.5 ± 4.7	27.4 ± 10.2	24.5 ± 7.2
99	16.4 ± 6.3	15.2 ± 5.1	28.3 ± 9.4	24.0 ± 8.0
100	13.4 ± 3.6	12.8 ± 3.5	21.5 ± 6.4	19.0 ± 5.3
101	10.6 ± 3.7	12.5 ± 3.4	18.3 ± 6.4	19.9 ± 5.2
102	16.6 ± 7.7	16.5 ± 5.7	26.8 ± 12.5	25.7 ± 10.3
107	14.5 ± 5.7	13.6 ± 6.0	23.8 ± 9.2	20.4 ± 8.9
Mean ± SD	14.7 ± 2.5	14.0 ± 1.4	24.6 ± 4.1	21.8 ± 2.7
P value[(b)]	*0.0048*	*0.0011*	*0.0022*	*0.0012*

SD = Standard Deviation

[(a)] t-test values for comparison between VT glaucoma group and normal group

[(b)] t-test values for comparison between MT glaucoma group and VT glaucoma group

Table 2

Dendrite complexity and total dendrite length of vehicle-treated and memantine-treated glaucoma monkeys

	% Decrease in dendrite complexity, Mean		% Decrease in total dendrite length, Mean	
Group, ID	**Layer 1**	**Layer 6**	**Layer 1**	**Layer 6**
Vehicle-treated				
91	51.9	48.6	52.2	51.6
92	59.9	55.2	57.9	55.5
93	55.3	55.7	56.4	59.9
96	55.7	49.5	51.4	46.3
98	50.6	41.5	50.6	46.6
105	48.5	44.8	50.1	48.4
106	48.5	39.6	47.8	44.2
Mean ± SD	52.9 ± 4.2	47.8 ± 6.3	52.4 ± 3.6	50.4 ± 5.7
Memantine-treated				
94	23.2	31.1	22.9	32.9
95	49.4	40.6	45.5	44.8
97	34.2	31.6	28.8	27.3
99	30.8	28.3	26.5	28.8
100	43.5	39.6	44.2	43.6
101	55.3	41.0	52.5	40.9
102	30.0	22.2	30.4	23.7
107	38.8	35.8	38.2	39.5
Mean ± SD	38.1 ± 10.7	33.8 ± 6.7	36.1 ± 10.5	35.2 ± 8.1
P value	*0.0047*	*0.0011*	*0.0019*	*0.0011*

SD - Standard Deviation